

Highly sensitive tuning of coupled optical ring resonators by microfluidics

Siyka I. Shopova · Yuze Sun · A. T. Rosenberger · Xudong Fan

Received: 1 August 2008 / Accepted: 10 November 2008 / Published online: 26 November 2008
© Springer-Verlag 2008

Abstract The authors develop optofluidic coupled ring resonator (OCR) system in which one of the ring resonators serves as a microfluidic channel. Highly sensitive tuning of the OCR is demonstrated by making small changes in the refractive index of the fluid. A refractometric sensing scheme using the OCR is proposed and demonstrated, allowing for measuring a refractive index change down to 10^{-9} refractive index units, two orders of magnitude better than a single ring resonator.

Keywords Coupled resonators · Microfluidics · Sensing

1 Introduction

Work on coherently coupled optical ring resonators is of interest because it is promising for applications such as optical delay lines (Maleki et al. 2004; Xu et al. 2006, 2007; Sandhu et al. 2007; Yanik and Fan 2007), filtering (Maleki et al. 2004; Paloczi et al. 2005), optical buffers (Yanik et al. 2004; Mario and Chin 2008), gyroscopy (Scheuer and Yariv 2006), and sensing (Chao and Guo 2003; Kurt and Citrin 2005; Passaro and De Leonardi 2006; Xiao et al. 2008). Each of these applications requires achieving a very particular state of interference, and therefore, the ability to tune

the coupled resonator system is imperative. Tuning can be achieved through several different mechanisms: (1) changing the coupling strength between the resonators or between the waveguide and the adjacent resonator (Maleki et al. 2004; Naweed et al. 2005; Totsuka et al. 2007); (2) changing the internal losses in the coupled resonators (Sandhu et al. 2007); (3) photobleaching chromophores doped in polymer waveguides (Scheuer et al. 2005); and (4) detuning the resonances from each other, which has been achieved by changing the refractive index (RI) in one of the resonators utilizing temperature control or the free carrier dispersion effect (Xu et al. 2006, 2007). Changing the RI to detune one resonance can also be accomplished by optofluidics, which takes advantage of the adaptiveness of liquids for various configurations and their large RI tuning range (Psaltis et al. 2006). In fact, optofluidic tuning of a single ring resonator on a chip was recently demonstrated for filtering (Levy et al. 2006). However, liquid tuning of the coupled ring resonators has not yet been explored. Although standard techniques are readily available for fabricating the coupled ring resonator systems on a chip, individually tuning one of the resonators is challenging.

2 Methods

Here, we develop an optofluidic coupled ring resonator (OCR) system that enables liquid tuning of the resonance. The OCR system consists of two fused silica capillaries placed in close proximity as shown in Fig. 1a. The circular cross section of a capillary supports whispering gallery modes (WGMs). One of the capillaries has a thin wall (3–5 μm) and serves as a microfluidic channel. Since the wall is thin, the WGM spectral position and hence the interference state of the coupled ring resonator can be

S. I. Shopova · Y. Sun · X. Fan (✉)
Biological Engineering Department,
University of Missouri, Columbia,
MO 65211, USA
e-mail: fanxud@missouri.edu

A. T. Rosenberger
Department of Physics, Oklahoma State University,
Stillwater, OK 74078, USA

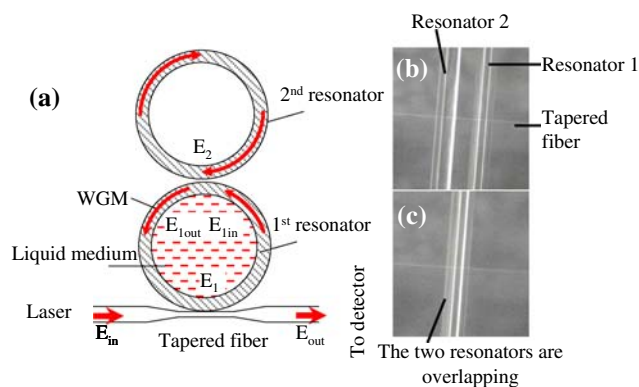


Fig. 1 **a** A schematic of the experimental setup. **b** A picture of the two capillaries and the tapered fiber; Resonator 2 is slightly above and aside of Resonator 1, which is in contact with the tapered fiber. **c** Top view of the two resonators brought in contact

tuned by the liquid passing through this capillary (White et al. 2006). The OCRR provides an excellent liquid-tunable model system consisting of dielectric resonators (rather than semiconductor-based resonators) with extremely high Q -factors ($>10^7$), which is very difficult to realize with an on-chip coupled ring resonator system. The high Q -factor is important for achieving longer storage time in delay lines (Yanik and Fan 2007), sharper dips for filtering (Maleki et al. 2004), and longer effective optical path length for sensing. In turn, because the changes in the interference state of coupled resonators are indicative for changes in the intrinsic parameters such as RI and the absorption loss, the OCRR can also provide a platform for bio-chemical sensing, whose performance is further enhanced by its microfluidic nature. In this work, we experimentally investigate the liquid tuning of the state of the OCRR by changing the effective RI in one of the resonators. Results are in excellent agreement with the simulations that show a measurable change in the interference state produced by as little as a 10^{-9} change of the effective RI. The possibility of using this OCRR system as a sensitive refractometric sensor will also be discussed.

The experimental setup is illustrated in Fig. 1a, with the corresponding picture shown in Fig. 1b and c. A thin-walled ($\sim 4 \mu\text{m}$) capillary of $115 \mu\text{m}$ in outer diameter (OD) serves as a microfluidic channel. It is placed in contact with a tapered fiber on one side and with a thick-walled ($\sim 12 \mu\text{m}$ in wall thickness) capillary of the same size on the other side. The liquid is pumped with a peristaltic pump. Light from a $1,550 \text{ nm}$ tunable diode laser is coupled into the OCRR system via the tapered fiber and detected at the distal end of the fiber.

Interference between co-resonant WGMs in the two ring resonators often results in mode splitting (Smith et al. 2003). The power transmitted through the taper can be described by:

$$\left| \frac{E_{out}}{E_{in}} \right|^2 = \left| \frac{r_1 - e^{-\frac{\alpha_1 l_1}{2}} e^{i\delta_1} \Theta(\delta_2, \alpha_2)}{1 - r_1 e^{-\frac{\alpha_1 l_1}{2}} e^{i\delta_2} \Theta(\delta_2, \alpha_2)} \right|^2, \quad (1)$$

where

$$\Theta(\delta_2, \alpha_2) = \frac{E_{1out}}{E_{1in}} = \frac{r_2 - e^{-\frac{\alpha_2 l_2}{2}} e^{i\delta_2}}{1 - r_2 e^{-\frac{\alpha_2 l_2}{2}} e^{i\delta_2}} \quad (2)$$

is the complex electric field transmission for a single ring resonator coupled to a waveguide. $\delta_i = \frac{2\pi n_i^{\text{eff}} l_i}{\lambda}$ is the round trip phase shift. l_i is the circumference of the ring, and λ is the wavelength. $i = 1, 2$ denotes either Resonator 1 or 2. n_i^{eff} is the effective RI of each ring. α_i is the absorption coefficient. r_1 and r_2 are the reflection coefficients between waveguide and Resonator 1 and between Resonator 1 and Resonator 2, respectively.

3 Results and discussion

The design shown in Fig. 1 allows for continuous change in the OCRR system by running a mixture of water and ethanol through Resonator 1, which varies n_1^{eff} and hence the resonance of Resonator 1. The bottom curve in Fig. 2a shows the modes of Resonator 1 filled with water in the absence of Resonator 2. Using the method described in our previous work, in which the WGM spectral shift is monitored as the core RI is increased (White et al. 2006), we determine that Resonator 1 has a wall thickness of $4.5 \mu\text{m}$ and the co-resonant mode in Resonator 1 (the right mode in Fig. 2a) is the second radial order WGM with 0.18% fractional power in the core. Upon contact with Resonator 2, one mode in Resonator 1 remains intact, whereas the other mode, i.e., the co-resonant mode, exhibits splitting, since the two capillaries are not completely identical and not all the modes in Resonator 1 are co-resonant with Resonator 2. The quality factor (Q) of the co-resonant mode before splitting is 1.1×10^6 and the Q -factors of the modes of Resonator 2 only are 10^7 or greater. The thick-walled capillary (Resonator 2) is kept empty in this experiment. Upper curves show the progression of the split state of the OCRR as ethanol concentration is increased, changing the RI in the core by 1.384×10^{-4} to 1.66×10^{-3} RIU (refractive index units). This change in the core RI produces an effective RI change in Resonator 1, Δn_1^{eff} , from 2.5×10^{-7} to 3×10^{-6} RIU. The change in state of the coupled resonators is caused only by the change of the RI in the liquid core, which is supported by the comparison with the calculated curves in Fig. 2b based on Eqs. (1) and (2), in which the resonator loss, i.e., the Q -factor and the reflection coefficients r_1 and r_2 remain constant.

Since the split state depends on the difference of the optical paths in the two resonators as well as the coupling, it is possible to generate different interference states by

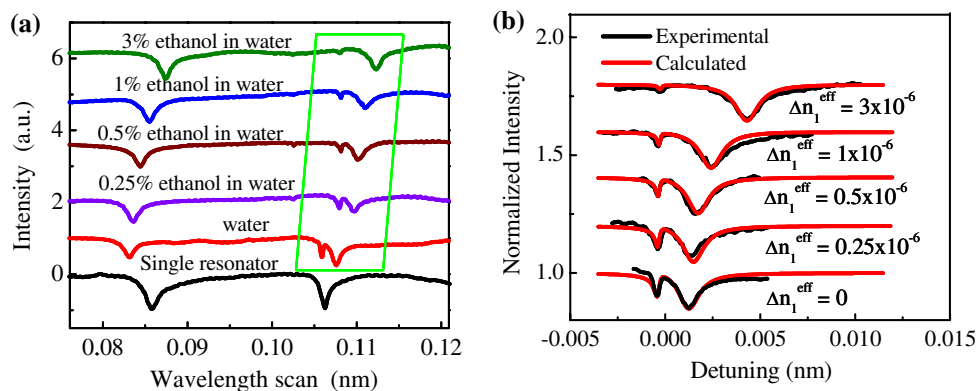
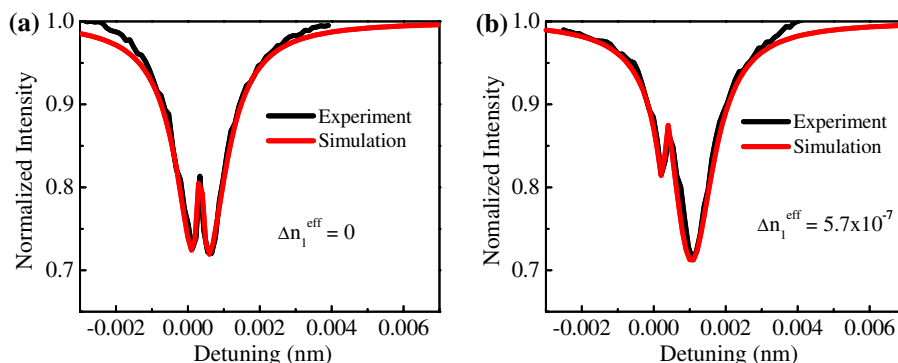


Fig. 2 **a** Wavelength scans of the OCRR as the RI of the liquid core of Resonator 1 is changed. Bottom scan shows un-split modes of Resonator 1 only. **b** Comparison between the experimental and

theoretical plots of the split mode for various effective RI changes in Resonator 1. $OD_1 = OD_2 = 115 \mu\text{m}$. $Q_1 = 1.1 \times 10^6$, $Q_2 = 1.1 \times 10^7$, $r_1 = 0.99996$, $r_2 = 0.9999997$, $n_1^{\text{eff}} = 1.44000112$, $n_2^{\text{eff}} = 1.44$

Fig. 3 Modes of the same OCRR system under different coupling conditions. The mode in (a) is formed when Resonator 1 is filled with water and the mode in (b) when Resonator 1 is filled with mixture of water and 0.25% ethanol. $r_1 = 0.999918$, $r_2 = 0.99999996$, $n_1^{\text{eff}} = 1.44000003$. Other parameters are the same as in Fig. 2



sliding Resonator 1 with respect to Resonator 2, because of slight differences in their radii and wall thickness and slightly different coupling. Figure 3 shows a split mode of the OCRR, as Resonator 2 is moved relative to Resonator 1. Figure 3a represents the initial split state as Resonator 1 is filled with water and Fig. 3b shows the state after adding 0.25% ethanol to the water. As in Fig. 2, we still use the second radial order WGM in Resonator 1. However, our characterization shows that the fractional light is increased to 0.4% due to the slightly decreased wall thickness (4.27 μm). The results in Figs. 2 and 3 show that the interference state of coupled resonators can be tuned with high precision by dynamic change in microfluidics in one of the resonators.

We now discuss one important application of the OCRR, that is, using the interference state of the OCRR to monitor small RI changes in the core of Resonator 1. In Fig. 4a, we utilize the spectral separation of the split modes to indicate the changes in n_1^{eff} . The curves are generated using the theoretical model described earlier. Experimental data from the scans shown in Fig. 2 are also plotted, in excellent agreement with the theoretical calculation. For a comparison, Fig. 4a also plots the calculated linear WGM shift for

a single ring resonator (Resonator 1). Although for small Δn^{eff} the RI sensitivity of the mode separation is slightly lower than that in a single ring resonator and with the increased Δn^{eff} the two sensitivity curves virtually overlap, using the mode separation significantly increases the resolution by rejection of common-mode noise such as temperature induced RI and radius change in the ring resonator, which results in a WGM shift, but not a change in mode separation. The only residual thermal noise is caused by the temperature induced solvent RI change. This noise, however, can be compensated for by flowing the solvent through both capillaries. With all these noise reduction mechanisms implemented, the detection limit will ultimately be determined by the spectral linewidth of the tunable diode laser ($\sim 1 \text{ MHz}$). Considering that the RI sensitivity for n_1^{eff} of 1,000 nm/RIU obtained from Fig. 4a and the laser spectral resolution of approximately 1 fm (one tenth of the laser linewidth), we estimate the detection limit to be on the order of 10^{-9} RIU. Note that if Δn^{eff} is sufficiently large (not shown in curve), the two ring resonators are decoupled, in which case, the OCRR refractometric result will follow that of a single resonator (Resonator 1).

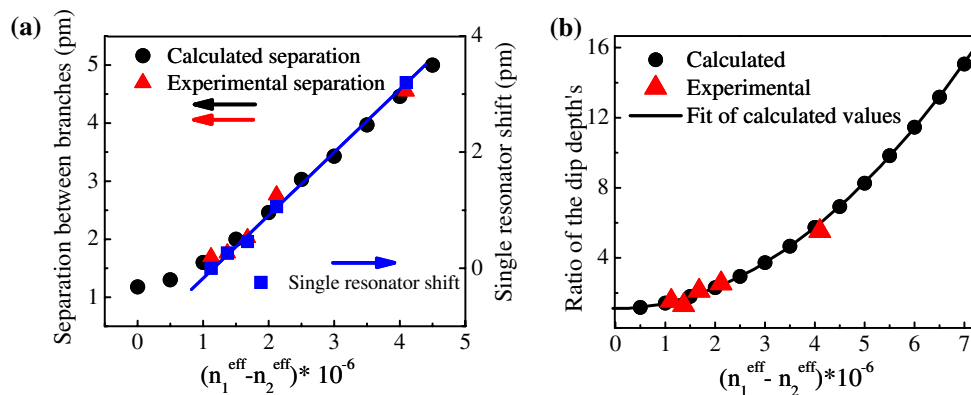


Fig. 4 **a** The calculated split mode separation (*circles*), experimental split mode separation obtained from Fig. 2b (*triangles*), and the single resonator WGM shift (*squares*) as a function of the difference in n^{eff} in the two resonators. Note that the split mode separation starts from the initial separation of 1.3 pm when Resonator 1 is filled with water

Figure 4b presents a new sensing mechanism that cannot be realized in a single ring resonator and that enables us to detect exceedingly small RI changes. In Fig. 4b, the change in the mode dip depth ratio (the larger dip depth is divided by the smaller depth) is used to indicate the change in n_1^{eff} . The RI sensitivity is determined by the slope of the curve in Fig. 4b. Our simulations show that the RI sensitivity, for a given structure, is the highest when the split modes have a dip depth of 0.5 (50% coupling,) at zero detuning (dip depth ratio = 1). The RI sensitivity can also be increased by increasing the Q -factor of Resonator 1. Figure 5a compares the calculated ratio for three different OCRRs. For all curves r_1 and r_2 are chosen such that both split modes have 50% coupling at zero detuning. Curve 1 in Fig. 5 shows RI sensitivity nearly 20 times higher than that in Fig. 4b when the Q -factor of Resonator 1 (Q_1) increases. Further increase in sensitivity is achieved by improving Q_1 from 8×10^6 to 10^7 , as shown by Curve 2 in Fig. 5. Curve 3 shows a significant increase of sensitivity as Q_1 reaches 10^8 . In practice, however, such a high Q -factor is difficult to achieve in Resonator 1 as solvent generally has strong optical absorption. One way to circumvent this problem is to use Resonator 2 as the microfluidic channel for which the wall of Resonator 2 needs to be thinned for sufficient solvent RI sensitivity. This will result in a much lower Q -factor (8×10^6) for the mode of this resonator, but will allow significant increase of the Q -factor for Resonator 1. In this case, the positions of the two branches of the coupled mode reverse, but the ratio of their depths remain the same.

For the OCRR structure, with parameters corresponding to the upper curve in Fig. 5, a change of $\Delta n^{\text{eff}} = |n_1^{\text{eff}} - n_2^{\text{eff}}|$ as small as 10^{-9} RIU causes a 1.24% change of the depth ratio. As mentioned earlier the thermal noise in OCRR can be compensated for to a great degree and the

whereas the spectral shift of Resonator 1 starts from zero. **b** Ratio of the mode dip depths, calculated (*circles*) and experimental (*triangles*), as a function of the difference in n^{eff} in the two resonators. Simulation parameters are the same as in Fig. 2

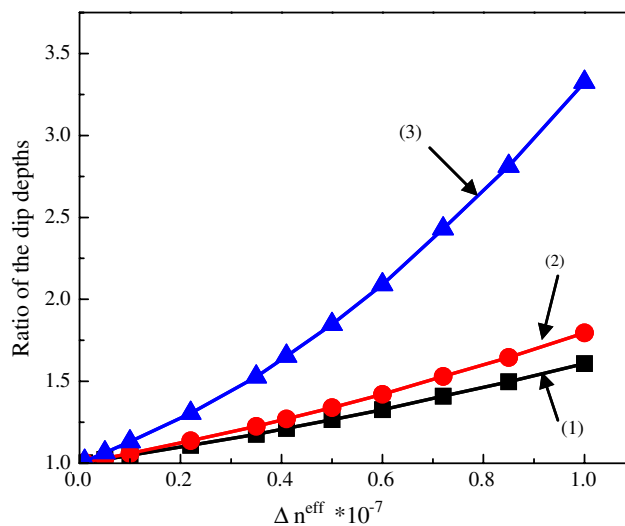


Fig. 5 Changes in the ratio of the dip depths as a function of the change in the effective RI in the microfluidic channel for a mode of 50% coupling (before detuning). *Curve 1* $Q_1 = 8 \times 10^6$, $Q_2 = 10^7$. *Curve 2* $Q_1 = 10^7$, $Q_2 = 10^7$. *Curve 3* $Q_1 = 10^8$, $Q_2 = 8 \times 10^6$

detection limit, i.e., the change in the dip depth's ratio, will be determined by the amplitude noise in the acquisition system (detector's noise, laser relative intensity noise, etc.). The relative error in intensity measurements of the current experimental results, shown in Fig. 6, is approximately 0.3% (for a critically coupled mode). This results in about 1% precision in the measured dip depth ratio for a 50% coupled mode. Therefore, our OCRR system is capable of detection the effective RI changes down to 10^{-9} RIU. For a comparison, in conventional single fused silica ring resonator-based refractometric sensors, the temperature induced WGM shift is approximately 10 pm/K at 1,550 nm (Suter et al. 2007), which leads to a detection limit for Δn^{eff} of approximately 1×10^{-7} RIU when the temperature is

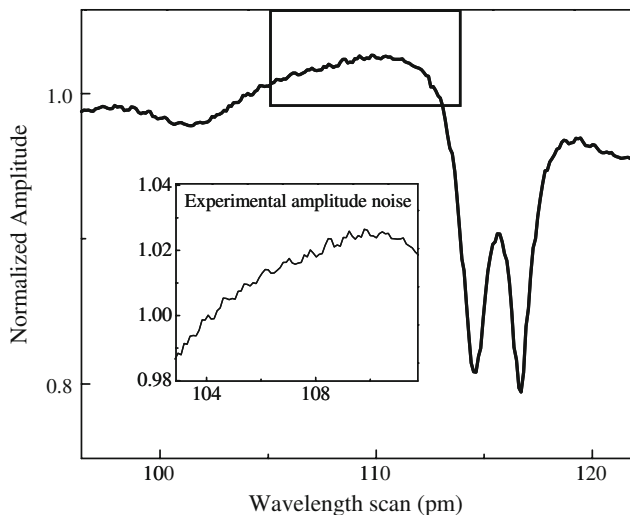


Fig. 6 A wavelength scan of a split mode showing the amplitude noise in the experimental measurements

stabilized within 0.01 K. It should be pointed out that the detection limit of the OCRR can be further improved by using a laser light with a wavelength at which the solvent in the microfluidic channel is not absorbing, thus increasing the Q -factor of the mode in Resonator 1, and by applying filtering techniques such as lock-in amplification to suppress the noise.

In summary, we have shown sensitive liquid tuning of the OCRR system by changing the RI of one of the ring resonators. We also proposed a refractometric sensing scheme in which the OCRR is capable of detecting the effective RI change as low as 10^{-9} RIU, two orders of magnitude improvement over the single ring resonator.

Acknowledgments The authors acknowledge the support from the Wallace Coulter Foundation Early Career Award and National Science Foundation-CAREER (CBET-0747398).

References

- Chao CY, Guo LJ (2003) Biochemical sensors based on polymer microrings with sharp asymmetrical resonance. *Appl Phys Lett* 83:1527–1529
- Kurt H, Citrin DS (2005) Coupled-resonator optical waveguides for biochemical sensing of nanoliter volumes of analyte in the terahertz region. *Appl Phys Lett* 87:241119
- Levy U, Campbell K, Groisman A, Mookherjea S, Fainman Y (2006) On-chip microfluidic tuning of an optical microring resonator. *Appl Phys Lett* 88:111107
- Maleki L, Matsko AB, Savchenkov AA, Ilchenko VS (2004) Tunable delay line with interacting whispering-gallery-mode resonators. *Opt Lett* 29:626–628
- Mario LY, Chin MK (2008) Optical buffer with higher delay-bandwidth product in a two-ring system. *Opt Express* 16:1796–1807
- Naweed A, Farca G, Shopova SI, Rosenberger AT (2005) Induced transparency and absorption in coupled whispering-gallery microresonators. *Phys Rev A* 71:043804
- Paloczi GT, Scheuer J, Yariv A (2005) Compact microring-based wavelength-selective inline optical reflector. *IEEE Photonics Technol Lett* 17:390–392
- Passaro VMN, De Leonardis F (2006) Modeling and design of a novel high-sensitivity electric field silicon-on-insulator sensor based on a whispering-gallery-mode resonator. *IEEE J Selected Top Quantum Electron* 12:124–133
- Psaltis D, Quake SR, Yang C (2006) Developing optofluidic technology through the fusion of microfluidics and optics. *Nature* 442:381–386
- Sandhu S, Povinelli ML, Fan S (2007) Stopping and time reversing a light pulse using dynamic loss tuning of coupled-resonator delay lines. *Opt Lett* 32:3333–3335
- Scheuer J, Yariv A (2006) Sagnac effect in coupled-resonator slow-light waveguide structures. *Phys Rev Lett* 96:053901
- Scheuer J, Paloczi GT, Yariv A (2005) All optically tunable wavelength-selective reflector consisting of coupled polymeric microring resonators. *Appl Phys Lett* 87:251102
- Smith DD, Chang H, Fuller KA (2003) Whispering-gallery mode splitting in coupled microresonators. *J Opt Soc Am B Opt Phys* 20:1967–1974
- Suter JD, White IM, Zhu H, Fan X (2007) Thermal characterization of liquid core optical ring resonator sensors. *Appl Opt* 46:389–396
- Totsuka K, Kobayashi N, Tomita M (2007) Slow light in coupled-resonator-induced transparency. *Phys Rev Lett* 98:213904
- White IM, Oveys H, Fan X (2006) Liquid-core optical ring-resonator sensors. *Opt Lett* 31:1319–1321
- Xiao YF, Gaddam V, Yang L (2008) Coupled optical microcavities: an enhanced refractometric sensing configuration. *Opt Express* 16:12538–12543
- Xu Q, Shakya J, Lipson M (2006) Direct measurement of tunable optical delays on chip analogue to electromagnetically induced transparency. *Opt Express* 14:6463–6468
- Xu Q, Dong P, Lipson M (2007) Breaking the delay-bandwidth limit in a photonic structure. *Nat Phys* 3:406–410
- Yanik MF, Fan S (2007) Slow light—dynamic photon storage. *Nat Phys* 3:372–374
- Yanik MF, Suh W, Wang Z, Fan SH (2004) Stopping light in a waveguide with an all-optical analog of electromagnetically induced transparency. *Phys Rev Lett* 93:233903